Signal Generation Model for High Density Magnetic Recording

Aleksandar Kavčić and José M. F. Moura

Data Storage Systems Center, Carnegie Mellon University, Pittsburgh, PA 15213-3890

ABSTRACT—When designing magnetic recording detectors, we want them to be tuned to signal and noise characteristics of readback waveforms. Interest has arisen in creating realistic readback waveforms via computer simulation since this provides the designer with flexibility of quickly changing the recording parameters. We present here an efficient, stable and realistic zig-zag media transition model as a faster alternative to micromagnetic modeling. Our zig-zag model offers four orders of magnitude of computational savings over micromagnetic modeling. Due to this low computational complexity, it is well suited for applications in signal processing, where a large number of transitions needs to be created. We show how to set the parameters of the model to describe high density recording phenomena. We also present a readback strategy for obtaining the readback signal. A simulation example shows the applicability of the model.

1. Introduction

In high density magnetic recording, readback detector designers are faced with a channel that deviates severely from a linear channel with additive Gaussian noise. The noise in magnetic recording is a combination of electronics additive noise and signal dependent transition noise. At low densities, transition noise exhibits itself as jitter. At high densities, neighboring magnetization transitions in the media react with each other causing further signal quality degradation. First, at close transition spacings, the currently written transition shifts towards the previously written one. This is called nonlinear transition shift (NLTS). Second, going from low to high recording densities, the media noise changes its character. It gains power and it also changes from jitter dominated to amplitude variation dominated. Third, at close transition separations, magnetization patterns have been observed to percolate through neighboring regions of opposite magnetization, causing partial signal erasure, also referred to as nonlinear amplitude loss (NLAS). While these are all products of the writing process, there are also unwanted effects produced by the reading process. The head sensitivity function of the read head has a finite width. As the read head flies over the magnetic medium, it senses a few adjacent transitions, causing intersymbol interference (ISI). Also, magnetoresistive (MR) read heads introduce further nonlinearities in the readback.

Ultimately, any detector needs to be tested on real data. However, testing on real data does not provide the flexibility of easily changing the system parameters, a step usually needed in the design process. It is advantageous to have an algorithm for generating high density signals via computer simulation. Micromagnetic models [1], [2], for example, are very accurate in predicting magnetization patterns, but they are too computationally complex for the generation of millions of transitions needed in error rate studies of a detector. On the other hand, simpler pulse amplitude modulation (PAM) type models [3]–[5] are faster, but they do not provide the necessary detail, particularly at high recording densities where adjacent transitions interact.

In this paper, we discuss a compromise between the two types of models. We believe that the signal generation model should mimic the actual recording process, but we reduce the computational complexity by capturing the essence of the recording process in only a few variables. The basic building block of the model is a random zig-zag line across the track representing a transition wall. We call the model the triangle zig-zag transition (TZ-ZT) [6], [7] model because the zig-zag line is constructed from lateral sides of isosceles triangles. Together with a readback model, this provides a simple but realistic recording process model, as we will show in this paper.

The paper is organized as follows. In Section 2, we shortly describe the idea behind stochastic zig-zag transition models and the TZ-ZT model. In Section 3, we show how to set the parameters of the model to describe each of the following: transition profile shape, jitter noise, nonlinear transition shift, high density media noise and partial erasure. We show how readback signals and readback electronics noise are obtained in Section 4. A modeling example is given in Section 5 to show the applicability of the model and to present comparison results between the TZ-ZT model and the micromagnetic model. Section 6 concludes the paper.

2. Stochastic zig-zag transition modeling

It has long been observed that the transition line separating two regions of different magnetization is not a straight line, but rather a zig-zag type shape similar to the one in Figure 1 [8], [9]. An early idea was to take Lorenz microscopy photographs of these zig-zag patterns [9] and from them determine the probability density function (pdf) of the sawtooth lengths and vertex angles, denoted by W_i and θ_i respectively in Figure 1. In [10], [11], this idea is taken a step further by fixing the angle θ to be a constant and finding a relationship between the pdf of the sawtooth lengths and a media hysteresis loop.

These early models have problems if they are going to be

This work was supported in part by the National Science Foundation under Grant No. ECD-8907068. The United States government has certain rights in this material.

0-7803-3336-5/96 $5.00 © 1996 IEEE

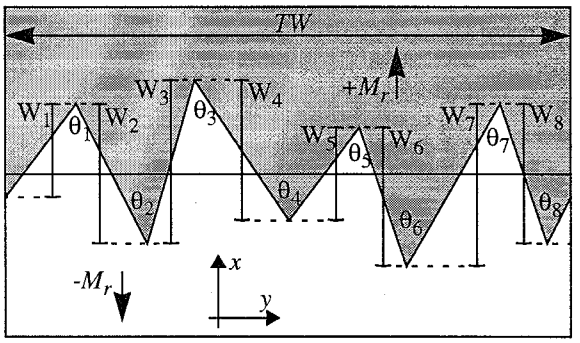

Fig. 1. Sawtooth (peak-to-peak) zig-zag model; x:down-track direction; y: cross-track direction.

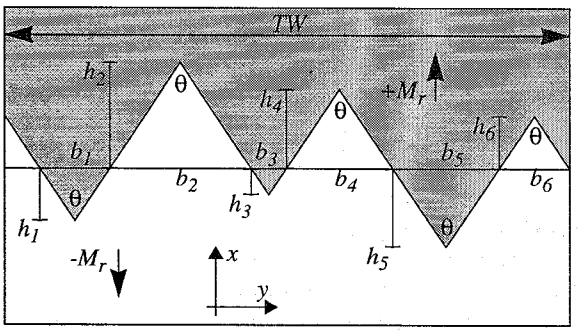

Fig. 2. Triangle zig-zag transition model; x:down-track direction; y: cross-track direction.

used for generating simulated transitions. If the sawtooth lengths are to be used as independent random variables, we get an independent increment random process [12], which exhibits instability due to a growing variance. This can be fixed by deconvolving the sawtooth pdf as in [13], but it still leaves the problem of determining the pdf of the sawteeth and the vertex angles. Taking Lorenz microscopy pictures is too complicated. On the other hand, if we use the approach in [10], [11], we need prior information about the vertex angle θ to determine the sawtooth pdf, and that is not always available.

Recently, renewed interest in expedient media models has arisen. Reference [14] discusses a microtrack type model. The track is broken into smaller tracks (microtracks) and each microtrack is assumed to hold a perfect transition. In contrast, our model is a zig-zag model, similar to the ones cited above, but in our formulation we avoid the problems encountered in [9]–[11], [13]. Our model is not an independent increment random process. Therefore it is stable, and there exist unique relationships between the defining quantities of the model and the recording parameters [7].

The model we use is a zig-zag random process, where the zig-zag line is constructed from lateral sides of isosceles triangles, see Figure 2. Each triangle has a height h_i and a constant vertex angle θ. The triangles alternate in orientation such that if the i-th triangle has its vertex on one side of the basis line (nominal transition location line), the $(i+1)$-st has it on the other side of the basis line. The heights h_i are drawn from a pdf $f_H(h)$. Because the model uses triangles as building blocks, we refer to it as the triangle zig-zag transition (TZ-ZT) model.

3. Modeling High Density Phenomena

In this section, we briefly overview how to set the TZ-ZT parameters in order to model the writing process at high recording densities. Proofs will not be given, we refer the reader to [6].

A. Transition profile

The first quantity we need to model is the correct transition profile of an isolated transition. If $M(x)$ denotes the down-track magnetization transition profile, with x denoting the down-track direction, on the average, we will have that same profile $M(x)$ in the TZ-ZT model if we set the pdf of the triangle heights to [6]

$$f_H(h) = \begin{cases} -\frac{M''(h)}{M'(0)} & \text{for } h \geq 0 \\ 0 & \text{for } h < 0 \end{cases} . \qquad (1)$$

Here we have assumed that $M(x)$ is an odd function and $M(x) > 0$ for $x > 0$. The superscript $'$ denotes the first derivative with respect to the down-track distance and $''$ denotes the second derivative.

B. Jitter noise

The cross-track correlation width is a media parameter that is directly related to the jitter variance [15]. Given a cross-track correlation width s of the media we are modeling, and knowing the pdf of the triangle heights $f_H(h)$, we achieve the same cross-track correlation width in the TZ-ZT model by setting the vertex angle to [7]

$$\theta = 2 \operatorname{atan}\left[\frac{s \cdot \mathrm{E}[H]}{2 \cdot \mathrm{Var}(H)}\right] . \qquad (2)$$

In (2), $\mathrm{E}[H]$ is the mean and $\mathrm{Var}(H)$ is the variance of the triangle heights H, which can be determined from the pdf $f_H(h)$.

C. Nonlinear transition shift (NLTS)

At close transition separations, the magnetostatic fields from the previously written transition cause the location of the transition currently being written to shift towards the previous transition. If the nominal spacing between transitions is B, then Bertram [15] has shown that the next transition appears closer to the first by

$$\Delta x = \frac{4 M_r \delta \left(d + \delta/2\right)^3}{\pi Q H_c B^3}, \qquad (3)$$

where M_r is the media remanent magnetization, δ is the media thickness, d is the flying height (magnetic spacing), Q is the head-field gradient factor and H_c is the media coercivity. To apply this formula, we first test how large B is and then write the next TZ-ZT transition closer to the previous one by Δx.

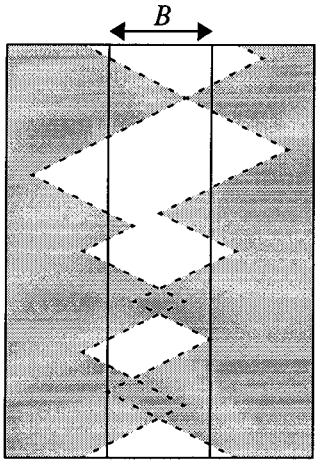

Fig. 3. Simple overlap percolation modeling.

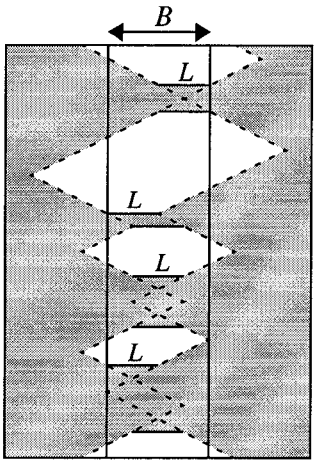

Fig. 4. Percolation when distance between zig-zags is less than L.

D. High density media noise

At high recording densities, in the region where neighboring transitions interact, the noise mechanism changes. For isolated transitions, jitter is the noise mechanism. At close transition separations, the noise gains power and the major noise mode becomes the amplitude variation [16], [17]. A way to model this is to use a result from [15], where it has been shown that the transition location variance in the x-direction (down-track direction) is larger than the variance for isolated transitions by a factor

$$\left(1 - \frac{8M_r\delta d^2}{\pi B^3 Q H_c}\right)^{-1}. \tag{4}$$

Implementing this into the TZ-ZT model means simply multiplying the triangle heights that are normally generated for an isolated transition by the square root of (4). In [7], we have shown that this gives rise to a nonlinear increase in media noise power and to the amplitude variation media noise mode.

E. Nonlinear amplitude loss (percolation)

Nonlinear amplitude loss occurs when magnetization patterns from neighboring transitions bridge through a domain of opposite magnetization. We model this phenomenon by letting the magnetization percolate wherever the adjacent zig-zags overlap, i.e., when the distance between adjacent zig-zags is less than 0, as illustrated in Figure 3. A better way to model percolation is to let the bridging occur wherever the distance between two adjacent zig-zags is less than some length L [14], [18], as illustrated in Figure 4.

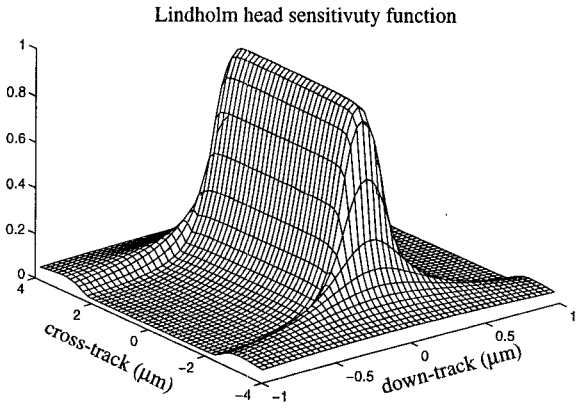

Fig. 5. Lindholm head sensitivity function.

4. Readback and Electronics Noise Modeling

A. Readback

The readback signal is obtained as the read head passes over a magnetized media. Analytically, the readback signal can be expressed as the convolution of the head sensitivity function and the magnetic charge in the media. In Figure 5, the head sensitivity function of a Lindholm head [19] has been plotted. In Figure 6, the Lindholm head sensitivity function has been placed over a zig-zag magnetic charge pattern and the response has been integrated in the cross-track direction to obtain the isolated readback pulse. For inductive readback, simple integration in the cross-track direction delivers the readback signal because inductive heads are linear transducers. Magnetoresistive heads are nonlinear transducers, and strictly speaking, linear superposition does not hold. However, if the MR element is perfectly biased, and the head is never taken into saturation, linear superposition matches the experimental data [20]. If there is severe nonlinearity in the readback, nonlinear superposition of flux contributions based on cross-track weighting can be applied [21].

B. Electronics noise

Adding the electronics noise is conceptually simple since the electronics noise can be considered to be white and Gaussian. However, as the readback signal as well as the noise pass through the preamplifier, this Gaussian noise becomes colored. Since the model presented thus far is a spatial model, we need to know (or make assumptions about) the disk rotating speed and the modulation code used in order to obtain the data rates and the required bandwidth of the preamplifier. We then assume the electronics noise to have a flat power spectral density (psd) in the preamplifier bandwidth. Integrating the psd in the bandwidth region gives us the electronics noise power. To obtain the electronics noise signal-to-noise ratio (SNR), we also need the absolute peak level (in Volts) of an readback isolated pulse. Both the psd and the readback voltage level depend

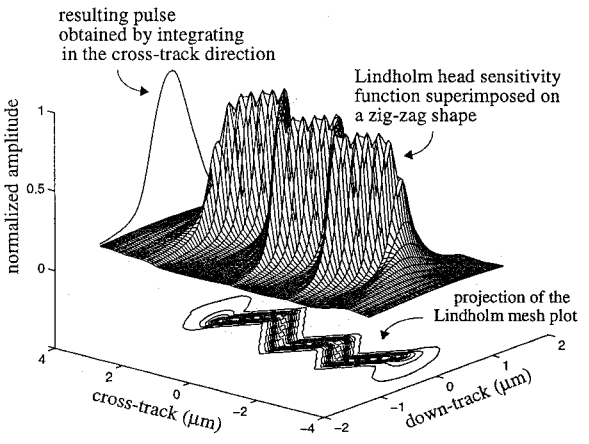

Fig. 6. Superposition of the zig-zag pattern and the Lindholm sensitivity function to obtain readback pulse.

on the head and preamplifier used. A good guess can be obtained if we pick the psd in the range 1 to $2\text{nV}/\sqrt{\text{Hz}}$ (including both the head and preamplifier noise) and the pulse peak in the range 0.1 to 2mV [22], [23].

5. Results

In this section we demonstrate through an example how the signal generating model works. We are using a Lindholm [19] inductive head with head width (track width) $TW = 4.8\mu$m, flying height $d = 0.1\mu$m and gap length $g = 0.28\mu$m, to read from a media with the following characteristics: remanent magnetization $M_r = 625\text{emu}/\text{cm}^3$, coercivity $H_c = 1670\text{Oe}$, media thickness $\delta = 400\text{Å}$ and orientation ratio O.R.= 1.3. These parameters were chosen such that we can compare our results with the experimental results obtained by other researchers [16], [17].

In order to determine the quantities defining the TZ-ZT model, the pdf $f_H(h)$ and the vertex angle θ, we ran the micromagnetic model 30 times to obtain 30 independent magnetization profiles $M_i(x)$, $i = 1, \ldots, 30$. Their average gave us a magnetization profile closely approximated by an error function

$$M(x) = \frac{1}{30}\sum_{i=1}^{30}\frac{M_i(x)}{M_r} \approx \text{erf}\left(\frac{x}{\sqrt{2}\sigma}\right), \qquad (5)$$

with $\sigma = 610\text{Å}$. Applying Equation (1) to this magnetization profile, we get the triangle heights pdf

$$f_H(h) = -\frac{M''(x)}{M'(0)} \approx \frac{h}{\sigma^2}\exp\left(-\frac{h^2}{2\sigma^2}\right) \quad \text{for} \quad h \geq 0, \qquad (6)$$

which is the well known Rayleigh pdf.

We next need to estimate the cross-track correlation width s in order to obtain the angle θ from Equation (2). First we calculate the empirical magnetization variance

$$\hat{\sigma}^2_M(x) = \frac{1}{30}\sum_{i=1}^{30}\left[\frac{M_i(x)}{M_r} - M(x)\right]^2. \qquad (7)$$

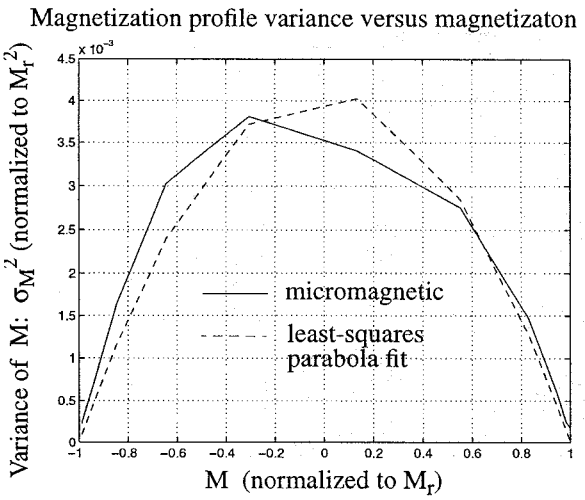

Fig. 7. Magnetization variance σ^2_M versus normalized magnetization M. Solid line – micromagnetic result. Dashed line – least squares parabola fit.

Ideally, if this variance were to be plotted against the magnetization $M(x)$, we would get a quadratic equation [24]

$$\sigma^2_M(x) = \frac{s}{TW}\left(1 - M(x)^2\right). \qquad (8)$$

Thus, by least-square fitting a parabola to the curve of $\hat{\sigma}^2_M(x)$ versus $M(x)$, we obtain the cross-track correlation width $s = 197\text{Å}$. Figure 7 shows the curve of $\hat{\sigma}^2_M(x)$ versus $M(x)$ and the least-squares parabola fit. We are now ready to apply equation (2). Notice that the triangle heights mean $\text{E}[H]$ and the variance $\text{Var}(H)$, for a Rayleigh random variable H with the pdf in (6), equal $\text{E}[H] = \frac{\sqrt{\pi}}{\sqrt{2}}\sigma$ and $\text{Var}(H) = \left(2 - \frac{\pi}{2}\right)\sigma^2$, where previously we determined $\sigma = 610\text{Å}$. With these parameters, Equation (2) yields $\theta = 50.7°$.

Having determined the TZ-ZT model quantities, we synthesized 50,000 independent TZ-ZT profiles and compared their statistics to 500 independent micromagnetic transitions. The comparison is depicted in Figures 8 and 9, where it is shown that the transition profiles and jitter histograms generated by TZ-ZT and by micromagnetic modeling match almost perfectly. We note that creating the 500 micromagnetic transitions took two weeks of CPU time on our workstation, while 50,000 TZ-ZTs were generated in about 2 hours.

We next study the characteristics of dibit recording for different transition separations. In this case we do not have results for the micromagnetic model since we need hundreds of independent dibits for each considered transition spacing. This takes months of computation. We present only the TZ-ZT results and use findings of other researchers to make a qualitative comparison.

For each distinct transition separation, we wrote 500 independent dibits and read them to obtain 500 voltage waveforms. After subtracting their mean, we were left with 500

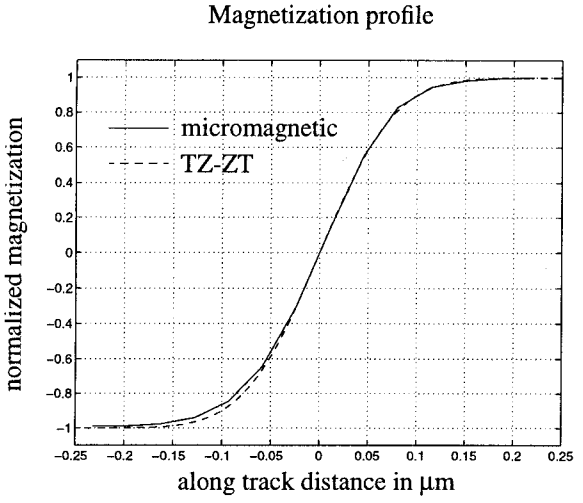

Fig. 8. Average magnetization profiles. Solid line - micromagnetic model. Dashed line - TZ-ZT.

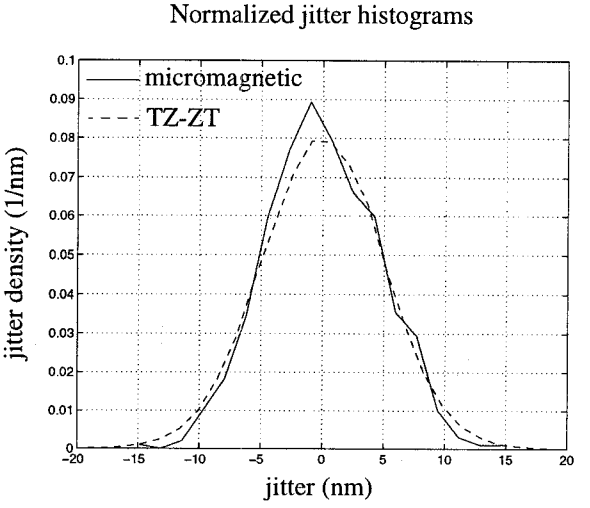

Fig. 9. Jitter histograms (normalized to unit area) - experimental jitter pdfs. Solid line - micromagnetic model. Dashed line - TZ-ZT

dibit media noise waveforms. We next calculated the autocorrelation function of the dibit media noise waveforms. Figure 10 and Figure 11 show the media noise autocorrelation functions for different transition spacings. In Figure 10, the media noise correlation function for a transition spacing of 0.7μm is shown. The arrows point to the positions where the pulse peaks would occur had the dipulse been plotted along the diagonal of the correlation function. Since the peaks of the correlation function do not coincide with the peak of the pulses, but are shifted both forward and backward, we recognize the signature of jitter noise. In Figure 11, the same correlation function is plotted, but the transition spacing is much lower at 0.2μm. Since the peaks of the correlation function now coincide with the peaks of the pulses, we recognize the signature of amplitude variation noise. Between these two transition separations (0.2μm and 0.7μm) is a region where peaks of the correlation function exist both at the pulse peak location as well as shifted, showing that there is a mixed contribution of both jitter and amplitude variation. Figures 10 and 11 match well experimental results in [25].

We decomposed each autocorrelation function into its principal components (the noise modes) using the Karhunen-Loeve decomposition (KLD). The KLD revealed that indeed two basic noise modes, the amplitude variations and jitter, dominate the dibit media noise. Their relative contribution to the total noise power changes with the dibit separation, as illustrated in Figure 12. We see that at large transition spacings, jitter dominates. As the transitions get closer, amplitude variations gain power, while the jitter power stays roughly the same. We conclude that the amplitude variation noise mode is mostly responsible for the superlinear noise power increase at high recording densities. These results are consistent with experimental findings [16],[17]. Figure 12 also shows how the dibit amplitude changes as a function of transition spacing. Both the linear dibit superposition amplitude and the actual dibit amplitude are shown normalized to the amplitude of an isolated pulse. In our simulations, we used $L = 0$ to model partial erasure. With $L > 0$, the amplitude drop would have been more severe.

6. Conclusion

In this paper, we presented a model for fast generation of realistic readback waveforms in longitudinal magnetic recording. The write process model is based on the triangle zig-zag transition (TZ-ZT) model. We also presented equations that relate the defining quantities of the model to phenomena occurring in high density magnetic recording, including jitter, nonlinear transition shift, high density media noise and partial signal erasure. We ran a signal generation example to show the applicability of the model, as well as to show comparison results between our model and the micromagnetic model. We observed that in modeling transition shapes and jitter noise for isolated pulses, TZ-ZT modeling and micromagnetic modeling are virtually identical, with the difference being that TZ-ZT modeling is 10^4 times faster than micromagnetic modeling. For interacting transitions (dibits), we were not able to make a comparison with micromagnetic modeling due to the enormous complexity of the micromagnetic model. Instead, we showed a qualitative match between the TZ-ZT modeling results and previously obtained experimental results.

References

[1] J.-G. Zhu and N. H. Bertram, "Micromagnetic studies of thin metallic films," *J. Appl. Phys.*, vol. 63, pp. 3248–3253, April 1988.

[2] J.-G. Zhu and N. H. Bertram, "Recording and transition noise simulations in thin film media," *IEEE Trans. Magn.*, vol. 24, pp. 2706–2708, Nov. 1988.

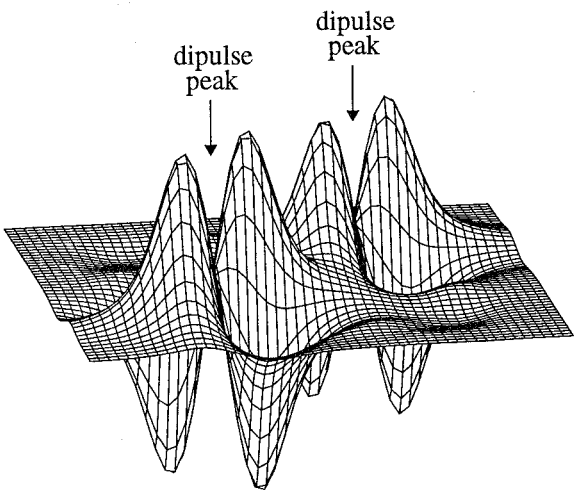

Fig. 10. Media noise autocorrelation function shape for transition spacing of 0.7μm. The arrows point to positions where pulse peaks occur.

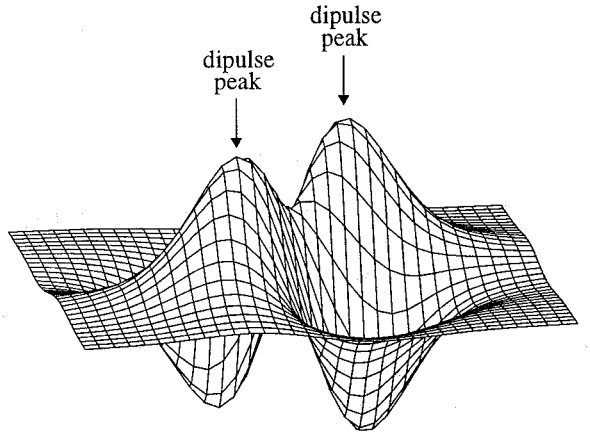

Fig. 11. Media noise autocorrelation function shape for transition spacing of 0.2μm. The arrows point to positions where pulse peaks occur.

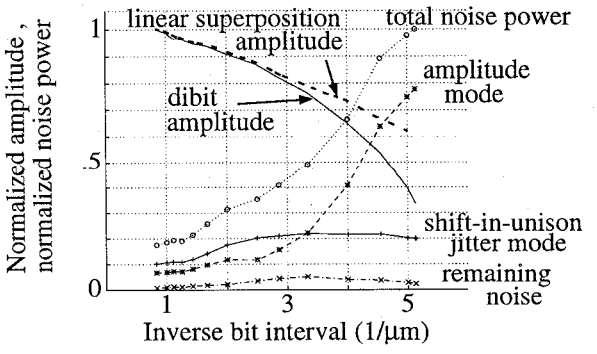

Fig. 12. Normalized dibit amplitude and normalized media noise mode powers as a function of inverse transition spacing.

[3] J. Moon, "Discrete-time modeling of transition-noise-dominant channels and study of detection performance," *IEEE Trans. Magn.*, vol. 27, pp. 4573–4578, Nov. 1991.

[4] S. K. Nair, H. Shafiee, and J. Moon, "Modeling and simulation of advanced read channels," *IEEE Trans. Magn.*, vol. MAG-29, pp. 4056–4058, Nov. 1993.

[5] L. C. Barbosa, "A model for magnetic recording channels with signal dependent noise," *IEEE Trans. Magn.*, vol. MAG-31, pp. 1062–1064, March 1995.

[6] A. Kavčić and J. M. F. Moura, "Triangle zig-zag transition modeling," tech. rep., Data Storage Systems Center, Dept. of Electrical and Computer Engineering, Carnegie Mellon University, Pittsburgh, PA, 1995. 54 pages.

[7] A. Kavčić and J. M. F. Moura, "Expedient media noise modeling: Isolated and interacting transitions," in *IEEE INTERMAG'96*, (Seattle), Apr. 1996.

[8] M. J. Freiser, "On the zigzag form of charged domain walls," *IBM J. Res. Dev.*, vol. 23, pp. 330–338, May 1979.

[9] T. C. Arnoldussen and H. C. Tong, "Zigzag transition profiles, noise, and correlation statistics in highly oriented longitudinal media," *IEEE Trans. Magn.*, vol. 22, pp. 889–891, Sept. 1986.

[10] B. K. Middleton and J. J. Miles, "Sawtooth magnetization transitions and the digital recording properties of thin film recording media," in *IEE Conf. Proc.*, pp. 20–25, April 1991.

[11] B. K. Middleton and J. J. Miles, "Recorded magnetization distributions in thin film media," *IEEE Trans. Magn.*, vol. 27, pp. 4954–4959, Nov. 1991.

[12] A. Papoulis, *Probability, Random Variables and Stochastic Processes.* New York: McGraw-Hill Book Company, 1965.

[13] Y.-S. Tang and L. Osse, "Zig-zag domains and metal film disk noise," *IEEE Trans. Magn.*, vol. MAG-23, pp. 2371–2373, Sept. 1987.

[14] J. Caroselli and J. K. Wolf, "A new model for media noise in thin film magnetic recording media," in *Proc. SPIE: Coding and Signal Processing for Information Storage*, vol. 2605, (Philadelphia), pp. 29–38, Oct. 1995.

[15] H. N. Bertram, *Theory of Magnetic Recording.* Cambridge: Cambridge University Press, 1994.

[16] J.-G. Zhu and H. Wang, "Noise characteristics of interacting transitions in longitudinal thin film media," *IEEE Trans. Magn.*, vol. 31, pp. 1065–1070, March 1995.

[17] J.-G. Zhu and X.-G. Ye, "Impact of medium noise on various partial response channels," *IEEE Trans. Magn.*, vol. 31, pp. 3087–3089, Nov. 1995.

[18] R. D. Brandt, A. J. Armstrong, H. N. Bertram, and J. K. Wolf, "A simple statistical model of partial erasure in thin film disk recording systems," *IEEE Trans. Magn.*, vol. MAG-27, pp. 4978–4980, Nov. 1991.

[19] D. A. Lindholm, "Magnetic fields of finite track width heads," *IEEE Trans. Magn.*, vol. 13, pp. 1460–1462, Sept. 1977.

[20] A. H. Sacks, *Position Signal Generation in Magnetic Disk Drives.* PhD thesis, Data Storage Systems Center, Dept. of Electrical and Computer Engineering, Carnegie Mellon University, Pittsburgh, PA, Sept. 1995.

[21] M. P. Vea, 1995. Quantum Corporation, Shrewsburry, MA; personal communication.

[22] T.-W. Pan and A. A. Abidi, "A wide-band CMOS read amplifier for magnetic data storage," *IEEE J. Solid-State Circuits*, vol. 27, pp. 863–873, June 1992.

[23] H. W. Klein and M. E. Robinson, "A $0.8\text{nV}/\sqrt{\text{Hz}}$ CMOS preamplifier for magneto-resistive read elements," *IEEE J. Solid-State Circuits*, vol. 29, pp. 1589–1595, Dec. 1994.

[24] H. N. Bertram and X. Che, "General analysis of noise in recorded transitions in thin film recording media," *IEEE Trans. Magn.*, vol. MAG-29, pp. 201–208, 1993.

[25] G. H. Lin, H. N. Bertram, and R. Simmons, "Noise correlations in dibit recording," *J. Appl. Phys.*, vol. 75, pp. 5765–5768, May 1994.